WIDEBAND SYNTHETIC-APERTURE IMAGING IN GROUND COORDINATES USING A DIGITAL PHASED-ARRAY TECHNIQUE

Geoffrey Shippey(1) and Tor Nordkvist(2)

(1) Dept. of Applied Electronics, Chalmers University of Technology, Göteborg
(2) now with Data Handling Dept. SAAB-Ericsson Space, Göteborg

1 INTRODUCTION

The paper describes a digital implementation of time-delay sonar beamforming for linear swept- frequency (chirp) sources. The technique, based on phase-shifting of match-filtered individual transducer echoes, is a direct equivalent of analog phased-array processing. The time-delays can be chosen to image any chosen array of pixels in the water column, or on the seabed, so a Cartesian image can be generated as easily as a polar image. In particular, if the platform position and orientation in space are known, the sonar image can be reconstructed in a stabilized ground coordinate system. A sequence of real aperture side-scan images can then be combined to form the synthetic- aperture image. Synthetic-aperture processing becomes simply an extension of real-aperture time-delay imaging.

A digital implementation of time-delay beamforming offers the advantage of area or volume image reconstruction without the need for special circuitry. However the problem arises that the required time-delays are not integral multiples of the sampling interval, so either inconveniently high sampling rates or some form of interpolation is needed. Several papers, eg [1,2,3] analyse the problem in terms of interpolating the echo samples ("up-sampling"). This paper will discuss interpolation of the match- filtered echoes rather than the samples themselves. This also reduces computational requirements considerably. Earlier papers from Heriot-Watt University outlined the method for narrow-band imaging [4,5], and recent research reported from Heriot-Watt describes experimental equipment [6]. The present paper extends the method to wideband echoes from a linear swept-frequency (chirp) source.

In order to reconstruct an image of all or part of an insonified sector, the transmission beamwidth must obviously exceed the receiver beamwidth. Hence the length and characteristics of the transmission and receiver arrays are generally very different. It will be shown that the azimuthal resolution obtainable from synthetic-aperture processing depends on the length of the transmission array, while the maximum displacement of the sonar platform between pings to suppress azimuthal ambiguities depends on the length of the receiver array. There are therefore advantages in using the maximum physical aperture available, in order to combine high resolution with rapid survey coverage.

A number of conditions must be satisfied to achieve true synthetic-aperture imaging - ping-to-ping phase coherence of the source and the medium, and repeatability of the platform positioning system within a fraction of the acoustic wavelength. These conditions become progressively harder to satisfy as the acoustic frequency increases, so synthetic aperture processing is not necessarily preferable for high-resolution survey. However a compromise solution is offerred by the phase-independant synthetic-aperture procedure discussed by Chatillon, Zakharia, and Bouchier in [7], and this is readily implemented using the digital phased-array technique. The method relies on a narrow sonar footprint in the range direction, which is most readily achieved using pulse compression with a chirp source. This could be an important additional reason for using wideband processing.

WIDEBAND SYNTHETIC-APERTURE IMAGING IN GROUND COORDINATES USING A DIGITAL PHASED-ARRAY TECHNIQUE

2 TIME-DELAY IMAGING BY QUADRATURE MATCH-FILTERING

The Phased-Array Approximation

Consider an idealised stationary 2D scene, with a linear array of N transducers, separated by a distance d, intercepting the acoustic wavefront rechoed from a reflector in the far field at (R, θ). In this simple model, a narrow-band source pulse $p(t) = A(t)\cos(2\pi ft)$, is projected from the centre of the array. The echo S_n received at the n'th transducer is an attenuated copy of $p(t)$, delayed by the two-way travel time T to the array centre, plus a differential delay to the transducer $\Delta T_n = nd\sin\theta/V$, where V is the speed of sound (assumed constant). Time-delay beamforming shifts each echo by $-\Delta T_n$ to bring the complete set into alignment. The composite signal:

$$S(t) = \sum_n w_n S_n(t - \Delta T_n) \tag{1}$$

is then formed, where the $\{w_n\}$ are array shading coefficients such as Tchebycheff [8] chosen to reduce side-lobe levels in the beam pattern. This composite signal gives constructive interference for echoes ariving from θ, and destructive interference otherwise. To image a target at $R = VT$ the delayed signal $S(t - T)$ is quadrature match-filtered with $P(t) = A(t)\exp(2\pi jft)$ to give the complex match-filtered signal:

$$U(T) = \int_{-L/2}^{L/2} P(u)\,S(u - T)\,du \tag{2}$$

The echo envelope is given by

$$I(R, \theta) = U(T)\,U^*(T) \tag{3}$$

For phased-array imaging, the transducer echo S_n is phase-shifted by $\alpha_n = -2\pi f\Delta T_n$ instead of time- delayed by $-\Delta T_n$. This brings the carrier-waveforms into phase to give the required constructive interference, but leaves the echo envelopes displaced from each other by ΔT_n. The result is an output pulse with envelope extended by t_{diff}, where $t_{diff} = Nd\sin\theta/V$ is the difference between the echo times for the nearest and farthest transducer in the array. For narrow-band signals, this time difference is usually negligible in comparison with the pulse length L so phased-array beamforming is a good approximation to true time-delay beamforming. Exchanging the order of summation and integration in (2) and writing $v_n = u_n + \Delta T_n$,

$$U(T) = \sum_n w_n \int_{-L/2}^{L/2} P(v_n - \Delta T_n)\,S_n(v_n - T)\,dv_n$$

Displacement of the limits can be neglected provided $T_n \ll L/2$, all n, and $A(v)$ vanishes at $\pm L/2$. Hence

$$U(T) = \sum_n w_n \exp(-2\pi jf\Delta T_n) \int_{-L/2}^{L/2} A(v_n - \Delta T_n)\exp(2\pi jftv_n)\,S_n(v_n - T)\,dv_n$$

$$\approx \sum_n w_n \exp(-2\pi jf\Delta T_n) \int_{-L/2}^{L/2} P(v)\,S_n(v - T)\,dv \tag{4}$$

WIDEBAND SYNTHETIC-APERTURE IMAGING IN GROUND COORDINATES
USING A DIGITAL PHASED-ARRAY TECHNIQUE

$$= \sum_n w_n exp\,(-2\pi jf\Delta T_n)\, U_n(T) \tag{5}$$

where $U_n(T)$ is the complex match-filtered n'th echo delayed by T. Thus the required phase-shift can be applied to the match-filtered transducer echoes rather than to the echoes themselves. (4) remains valid in the near field provided the computation of $\{\Delta T_n\}$ allows for the curvature of the echo wavefront.

Digital Phased-Array Beamforming

Now consider the discrete forms of the above equations. Assume that individual transducer echoes are sampled at interval τ and stored. The complex source becomes:

$$P(m) = A(m)\, exp\,(2\pi jmft)\,,\ m = -L/2 \ldots L/2-1 \tag{6}$$

In digital beamforming, echoes can be aligned within $\pm\tau/2$ by shifting an integral number of samples in store, so phase-shifting is only required to compensate for fractional time-delays. Let the required time delay for the n'th transducer be T_n, and let the nearest sample to this be delayed by t_n, so $T_n = t_n + \Delta t_n$ where Δt_n denotes the residual time delay. Then (4,5) become:

$$U(t) \approx \sum_n w_n exp\,(-2\pi jf\Delta T_n) \sum_{-L/2}^{L/2} P(m)\, S_n(m - t_n) \tag{7}$$

$$= \sum_n w_n exp\,(-2\pi jf\Delta t_n)\, U_n(t_n) \tag{8}$$

with the intensity $I(R,\theta)$ still given by (3). Eq (8) expresses the match-filtered composite signal as the weighted sum of phase-shifted, quadrature match-filtered, sampled echoes. For random R and θ, the residual time delays Δt_n are randomly distributed between $\pm\tau/2$ with equal probability. The peak of the compressed composite envelope is widened approximately by τ. The digital approximation (8) can be more accurate than the analog approximation (5) because the time-delays to be compensated by phase- shifting are less than $\pm\tau/2$, with τ chosen by the system designer. This is particularly important for the delay-sum implementation of synthetic-aperture processing (Section 4).

Rather surprisingly the same expression can be used if the source signature is a chirp pulse centred on f_c rather than a narrow-band signal. Fig.1a shows a 129 sample chirp pulse with Hanning envelope $e(m) = (1 + cos\,(2\pi m/L))/2$. Using frequencies normalised with respect to the sampling frequency, this chirp pulse spans one octave $f = 0.2 - 0.4$ with centre frequency $f_c = 0.3$. Fig.1b shows the centre samples of the compressed pulse envelope $\pm e(m)$, plus the in-phase and quadrature match-filtered source pulse $\pm ei(m)$ and $\pm eq(m)$. Fig.1c looks identical to Fig.1b, but in fact shows the modulated centre-frequency signals

$$ec(m) = e(m)\, cos\,(2\pi f_c m)\,,\ es(m) = e(m)\, sin\,(2\pi f_c m)\,.$$

The normalised rms difference between the match-filtered signal and the corresponding modulated centre frequency:

$$\sqrt{\frac{\overline{(ei(m) - ec(m))^2}}{\overline{ei(m)^2}}}$$

WIDEBAND SYNTHETIC-APERTURE IMAGING IN GROUND COORDINATES
USING A DIGITAL PHASED-ARRAY TECHNIQUE

is approximately 2%. A range of chirp pulse with Hanning envelopes was investigated, and this normalised difference was of the same order of magnitude for all the examples tested. Thus the in-phase and quadrature match-filtered chirp pulse are almost indistinguishable from the centre frequency waveforms modulated by the compressed envelope. As a further consequence, time delays to the matched-filtered signals are accurately approximated by phase- shifts calculated using the centre frequency f_c. Hence (8) remains valid with f replaced by f_c.

The same expression can be used for chirp pulses above Nyquist provided the normalised frequency range contains no multiple of 0.5. To allow for aliassing of the match-filtered signal, replace f_c by $-f_c$ in (8) if $0.5k < f_c < 0.5k + 0.5$ and k is odd.

Area Imaging

Digital processing can be used to form a 2D image, rather than a 1D beam. Since a different value of θ can be chosen for each R, a Cartesian image can be generated as easily as a polar image. Fig 2 shows the point-spread function derived using the Hanning pulse of Fig 1a with $\tau = 2\mu s$, $f_c = 150kHz$, and $\lambda_c = 1cm$ at a sound speed of 1500 m/sec. Fig.2 is of course a Cartesian image with a fine grid spacing. To generate the psf, the echo from an on-axis target at 50 m is received by a 1 m array of 32 elements spaced at $3\lambda_c$. The wide transducer spacing is deliberate, since the computational load is reduced by populating the receiver aperture as sparsely as possible. Grating lobes are supressed by limiting the insonification angle, in this case to $\pm 16^{\circ}$. Azimuthal beam-width is proportional to the acoustic wavelength, so for a chirp source the footprint is wider for the low frequency components of the chirp pulse than the higher. Hence a reduction in pulse compression could be expected at the azimuthal extremities of the psf, as well as a range displacement towards the transmitter. However neither of these effects appear significant with the one-octave pulse used, and spatial resolution is as expected for a time-delay imaging system with dynamic focus.

It is possible to reconstruct alternative images from the same dataset of stored samples, for example with different pixel spacing. A wider output pulse to span a coarser grid is achieved by replacing $P(m)$ in (7) by a kernel with a lower time-bandwidth product.

Doppler Shift and Selective Attenuation

If necessary, Doppler shift due to movement of the sonar platform or the target can be compensated by correcting the estimated 2-way time-delays for the velocity component along the line-of-sight to each pixel. The sampled waveform used for match-filtering must also be modified by the estimated Doppler shift. A single Doppler Shift applying to the whole imaged region present no problem, but there is a practical problem if different Doppler Shifts are required for different regions of the image since each transducer echo must then be match-filtered with each of the Doppler-shifted source signatures. The kernel can also be varied with echo-time to allow for selective attenuation of the transmitted pulse with frequency and range.

3 SIDE-SCAN GEOMETRY AND PIXEL-BASED IMAGING

Fig 3 shows a side-scan survey line in a North-Easterly direction, with XY representing the grid coordinate system. The survey is carried out by imaging each insonified point in the XY plane with a spacing of 10cm, 1m, etc forming a regular grid on the ground. Suppose that the seabed is locally flat and horizontal, at a known depth H below the sonar platform. Then each element in the grid can be imaged as a pixel by estimating the set of 2-way time delays from the projector to the centre of each grid-square and back to each element in the array. Assume that the acoustic projecter generates a fan- beam of beamwidth α. Then if the platform moves a distance of D between pings, there is continuous insonification of the seabed for all slant ranges greater than $D\alpha$ if pitch effects are neglected, so eventually all pixels will be scanned at least once as the platfrom moves through the water. For a properly stabilized image, time delays must also take roll and

WIDEBAND SYNTHETIC-APERTURE IMAGING IN GROUND COORDINATES USING A DIGITAL PHASED-ARRAY TECHNIQUE

pitch of the sonar platform into account, which also eliminates the pitch arteracts common on conventional side-scan records. The insonification boundary for each ping must be computed to avoid reconstructing image points in sonar shadow. This boundary must take account of platform attitude at the instant of transmission.

4 PHASE-DEPENDANT SYNTHETIC-APERTURE PROCESSING

The baseline of platform positions over which the same pixel is insonified increases with range. If each pixel point is imaged as long as it remains insonified, then synthetic-aperture processing becomes possible. Equation (8) above does not depend on how the transducers are mounted, or even whether the echoes are all received from the same transmitted pulse. The only requirement is that the source signature and the pixel location in space remain the same. Hence the synthetic-aperture formulation is identical to the real-aperture formulation. To generate the synthetic-aperture image, it is only necessary to average the complex values for each pixel derived from each real-aperture image over the number of pings for which the particular pixel remains insonified.

The correlation operation described in synthetic-aperture literature also corresponds to a delay-sum operation [9], so this form of SAS processing is not essentially different from real-aperture processing. However it is worth reviewing the resolution and azimuth aliassing aspects. Let $R(\theta)$, $T(\theta)$ be the beam patterns for the physical receive and transmit apertures. Suppose that the synthetic aperture at some range in the far field is given by $A = ND$ where D is the along-track platform movement between pings. Let L_R equal the length of the receiver aperture, with (for the moment) a narrow-band wavelength of λ. Then the synthetic aperture beam pattern, $Q(\theta)$, is given by

$$Q(\theta) = \sum_{n=-N/2}^{N/2} R(\theta)T(\theta)\,exp\,(-(4\pi jkD\sin\theta)/\lambda) \tag{9}$$

with 4π instead of 2π because of the two-way phase change with pixel-array separation. Hence

$$Q(\theta) = R(\theta)T(\theta)\sin\left[\left(\frac{1}{2}N+\frac{1}{2}\right)4\pi D\sin\theta/\lambda\right]/\sin\left[\frac{1}{2}\cdot 4\pi D\sin\theta/\lambda\right]$$

$$= R(\theta)T(\theta)\sin\left[2\pi A\sin\theta/\lambda\right]/\sin\left[2\pi D\sin\theta/\lambda\right] \tag{10}$$

giving azimuth ambiguities for $\sin\theta = k\lambda/D$, integer k. The unweighted beam-pattern for a continuous receiver array of length L_R is given by:

$$R(\theta) = \sin\left[\pi L_R\sin\theta/\lambda\right]/\left[\pi L_R\sin\theta/\lambda\right] \tag{11}$$

Combining (10) and (11) and setting $D = L_R/2$ [10] the ambigiuities are suppressed, leaving the beam pattern:

$$Q(\theta) = T(\theta)\sin\left[2\pi A\sin\theta/\lambda\right]/\left[\pi L_R\sin\theta/\lambda\right] \tag{12}$$

$Q(\theta)$ contains as a factor the beam-pattern for a real-aperture of length $2A$ regardless of the transmit beam pattern $T(\theta)$. This gives a nominal beamwidth of $\lambda/(2A)$, and a nominal along-track resolution of $(\lambda R)/(2A)$ at range R. The length of the synthetic aperture at range R is given by $A = R\alpha = \lambda R/L_T$ where L_T is the length of the transmitter aperture, so along-track resolution is $L_T/2$ independant of θ and R. Hence

WIDEBAND SYNTHETIC-APERTURE IMAGING IN GROUND COORDINATES
USING A DIGITAL PHASED-ARRAY TECHNIQUE

azimuth resolution depends on L_T, while D, the platform movement to suppress aliassing depends on L_R. By choosing a long receiver aperture, it is possible to achieve both high resolution and a high survey speed at the same time. If D varies for some reason, it is possible to vary the number of receiver transducers processed to maintain the relationship $D = L_R/2$ up to the physical length of the receiver aperture.

There are a number of approximations in the above analysis. Alias suppression is imperfect for reflectors which are not in the far-field [10]; the receiver transducers may be widely spaced to reduce the computation, and L_T will probably exceed λ/α for good sidelobe suppression. However these do not affect the main conclusions.

Fig 4a shows the simulated synthetic-aperture image corresponding to Fig.2 with a synthetic-aperture of length 30m, given by an insonification angle $\alpha = \pm 16°$. The physical aperture is moved 0.5m between pings, so 60 real-aperture images are used to construct the synthetic-aperture image. The diagonal artefacts corresponding to the insonifcation sector are due to uncompensated real-aperture contributions, and would be eliminated by applying one of the standard taper functions.

5 PHASE-INDEPENDANT SYNTHETIC-APERTURE PROCESSING

Phase-independant synthetic-aperture processing, termed envelope processing in [7], cannot improve azimuthal resolution to the same extent as is theoretically possible with phase-dependant synthetic- aperture processing. However it is much less demanding and could therefore be more effective at higher acoustic frequencies. Phase coherence and aliassing are irrelevant, and the required positioning accuracy is of the order of a few acoustic wavelengths rather than a fraction of the acoustic wavelength. Fig 5a,b shows the envelope-processed synthetic aperture image corresponding to Fig 4, using only five platform positions spanning the synthetic aperture rather than 60.

This image is virtually the same as superimposing the PSF from Fig 2 rotated through five incremental angles up to a total of $32°$. The simple model of rotating the real-aperture point-spread function can be used to estimate the azimuthal resolution obtainable with this method. Suppose the real-aperture psf is approximated by a bivariate normal distribution:

$$U(\rho, a) = exp-\left(\rho^2/\left(2\sigma_\rho{}^2\right) + a^2/\left(2\sigma_a{}^2\right)\right)$$

with variances σ_ρ, σ_a in the range and azimuth directions, and $\sigma_\alpha \gg \sigma_\rho$. Suppose also that this psf is evenly rotated through a total angle of α, with a sufficient number of samples superimposed to give a uniform distribution as a function of radial distance within the sector of angle α. Then the integral of U in the range direction $\int P(\rho, a)\, d\rho$ will be averaged out over an arc of length $a\alpha$, provided that $\alpha \gg \sigma_\rho$. Hence the resultant psf at radius a from the centre of the psf, and within the sector-angle α, is given by

$$U(a) \approx \sigma_\rho\sqrt{2\pi}/(a\alpha)\, exp\left(-a^2/2\sigma_a{}^2\right) \quad \text{for } \alpha \gg \sigma_\rho \tag{13a}$$

$$\rightarrow \quad \sigma_\rho\sqrt{2\pi}/(a\alpha) \quad \text{as } \alpha \rightarrow \infty \tag{13b}$$

The azimuth beamwidth is given by $U^2(a) = 1/2$, whence for $\sigma_a \gg \sigma_\rho$, $a = \sigma_\rho 2\sqrt{\pi}/\alpha$ independant of σ_a Thus azimuth resolution using phase-independant synthetic aperture processing is also independant of range in the far field. Now write $\alpha = \lambda_c/L_T$ where λ_c is the mid-frequency wavelength, and $\sigma_\rho = V/f_B$ where f_B is the chirp bandwidth. Then:

WIDEBAND SYNTHETIC-APERTURE IMAGING IN GROUND COORDINATES USING A DIGITAL PHASED-ARRAY TECHNIQUE

$$a = \frac{2\sqrt{\pi}V}{\lambda_c f_B} L_T = \frac{2\sqrt{\pi} f_c}{f_B} L_T \qquad (14)$$

For the one-octave chirp source in the example, $f_c/f_b = 2/3$, which gives $a \approx 2.5L_T$, compared with the corresponding figure of $0.5L_T$ for phase-dependant synthetic aperture processing. Too much notice should not be taken of the absolute value of an expression obtained using a very simplified model. However it is clear from the geometry and the above analysis that phase-independant SAS processing is most effective when resolution in the range direction is very good, which in turn means a high bandwidth as noted in [7]. However it should also be noted that the integrated psf outside the resolution cell steadily increases with range. For a distributed target, such as a seabed image, this accumulates to a significant level of background noise which will degrade the appearance of the image, reducing the contrast between bright reflectors and shadows.

6 IMAGE REGISTRATION

While this section is speculative, the subject matter is so closely related to imaging in ground coordinates that it would be unsatisfactory to omit it. Both phase-independant and phase-dependant techniques rely on precise registration of the physical-aperture images which combine to form the synthetic-aperture image. This creates a severe requirement for positioning repeatability along the length of the synthetic aperture. For phase-dependant SAS imaging, the random error must not exceed a fraction of the acoustic wavelength which becomes almost prohibitively difficult at mm wavelengths. Hence some method of automatic error correction is essential, often termed "auto-focus" in SAS literature. When the real-aperture images forming the synthetic aperture are generated in a ground coordinate system, auto-focus can be treated as the more familiar problem of image registration.

There is a considerable literature on registration of SAR image sequences using both correlation and optical flow techniques, for example [11,12]. Registration of sonar intensity (envelope) images to correct for positioning inaccuracies should be possible using similar techniques, probably using a selected region of each real aperture image, and avoiding far-field pixels which are degraded by electronic noise, and near-field pixels affected by steep grazing angles. A fine spacing of the pixel grid can be chosen for these selected windows to preserve the high spatial frequencies which are needed for precise registration.

Phase-dependant SAS processing requires the further step of registering the complex images derived from Equation (8) in phase. Consider first the related problem of compensating for phase variation of the transmitted pulse introducing an unknown constant phase-shift ϕ in all pixels of the reconstructed real-aperture image. Suppose $I_{ij} = A_{ij} + jB_{ij}$, $J_{ij} = C_{ij} + jD_{ij}$ are two complex images of the same scene derived from different platform positions, and we look for the phase shift ϕ to all the pixels of J which will minimises the difference between I and J. Then it is easily shown that ϕ is given by:

$$\tan\phi = \sum (AD - BC) / \sum (BD - AC)$$

where the sum is taken over all the ij. A similar procedure can be used to find across-track or along- track position errors if the consequent phase-shifts are resolved along the line-of-sight to each pixel. For the phase of each pixel to be useful for registration purposes, the sonar footprint must cover almost the same area when viewed from different platform positions, which is not the case using full pulse compression. Hence auxiliary real-aperture images must be generated for phase registration with similar range resolution to azimuth resolution in the selected regions.

WIDEBAND SYNTHETIC-APERTURE IMAGING IN GROUND COORDINATES
USING A DIGITAL PHASED-ARRAY TECHNIQUE

7 DISCUSSION

The paper has presented a rather straightforward technique for digital image reconstruction which extends readily to synthetic-aperture processing. Computational problems of wide-band processing are avoided by noting that the modulated centre-frequency of the pulse is a very good approximation to the match-filtered signal. For synthetic-aperture operation, there are distinct advantages in using a wide physical receiver aperture. This does not change the total computational load, but increases the maximum coverage rate and improves conditions for auto-focus estimation.

Self-registration of physical-aperture images generated in stabilized ground coordinates is a possible strategy for relaxing positioning accuracy requirements. "Poor-man's" SAS processing using the intensity image also deserves attention in this respect. These will be research priorities for the field experiments to be carried out in Sweden under the DAIM (Digital Acoustic Imaging) Project.

All the processing proposed in the paper has been based on a "locally flat seabed" assumption, which enables time delays to pixels lying on the seabed to be computed using the local height of the platform above it. For many interesting survey areas, this flat seabed assumption is far from satisfactory, so an important future research direction is to combine sector imaging described here with bathymetric estimation.

8 ACKNOWLEDGEMENTS

The research described here began in a project with Ron McHugh at the Dept of Computing and Control, Heriot-Watt University, Edinburgh, and informal collaboration has continued since that time. The research in Sweden reported is funded by the State Research Board NUTEK under the Rörliga Autonoma System (Robotics) Programme. Particular acknowledgement is expressed to DAIM colleagues, Peter Ulriksen (LTH), Ulf Bengtsson (Bofors Underwater Systems) and Olle Kröhling (Subvision AB) for creative discussions. Preparation of a MAST Proposal provided a valuable opportunity for contact with the LASSSO Research laboratory at CPE- Lyon, led by Manell Zakharia.

9 REFERENCES

1. R.G.Pridham and R.A.Mucci, "Digital interpolation beamforming for low-pass and band-pass signals", Proc.IEEE 67 (1979) pp.904-919
2. D.K.Peterson and G.S.Kino, "Real-time digital image reconstruction: a description of imaging hardware and quantization errors", IEEE Trans. Sonics Ultrason 31 237-251 (1984)
3. S.Ries "Digital time-delay beamforming with interpolated signals", Proc. European Conf. on Underwater Acoustics, ed. M.Weydert ,Elsevier, ECUA (Luxembourg 1992), pp.594-689
4. G.A.Shippey, R.McHugh, and J.G.Paul, "Digital holographic imaging for underwater acoustic applications", in Acoustical Imaging ed. H.Ermert and H-P Harjes (Plenum, New York 1992) Vol 19, pp867-872
5. J.G.Paul,R.McHugh, and G.A.Shippey, "Simulation study of a novel digital focussed beamformer for directly sampled bandpass signals,IEE Conf. on Sonar Signal Processing, Loughborough (Dec.1991)
6. R.McHugh, S.Shaw, N.Taylor, "A general-purpose digital focussed sonar beamformer", IEEE "Oceans" Conf. (Brest Sept. 1994) Vol I pp.229-234
7. J.Chatillon, M.E.Zakharia, and M.E.Bouchier, "Wideband synthetic aperture sonar: advantages and limitations" Proc.European Conf. on Underwater Acoustics, ed. M.Weydert ,Elsevier, ECUA (Luxembourg 1992), pp.709-712
8. R.O.Nielsen, Sonar Signal Processing, (Artech House, Boston, 1991)
9. M.P.Hayes and P.T.Gough, "Broad-band synthetic-aperture sonar", IEEE J.Oceanic Eng. OE-17 80-94 (Jan 1992)
10. K.D.Rolt and H.Schmidt, "Azimuthal ambiguities in synthetic aperture sonar and synthetic aperture radar imagery" IEEE J.Oceanic Eng. OE-17 73-79 (Jan 1992)
11. Y.Sun "Automatic ice motion retrieval from ERS-1 SAR images using the optical flow technique", Int.J.of Remote Sensing (in press)
12. R.Kwok, J.C.Curlander, R.McConnell, W.Kober and S.S.Pang,"Correlation and dynamic time warping: two methods for tracking ice floes in SAR images", IEEE Trans. on Geoscience and Remote Sensing, 29 No 6 (1991) pp.1004 1012

WIDEBAND SYNTHETIC-APERTURE IMAGING IN GROUND COORDINATES USING A DIGITAL PHASED-ARRAY TECHNIQUE

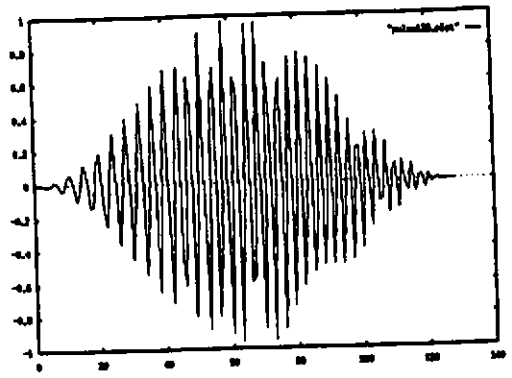

Fig 1a.129-sample chirp pulse with Hanning envelope, f=0.2-0.4 (normalised frequency)

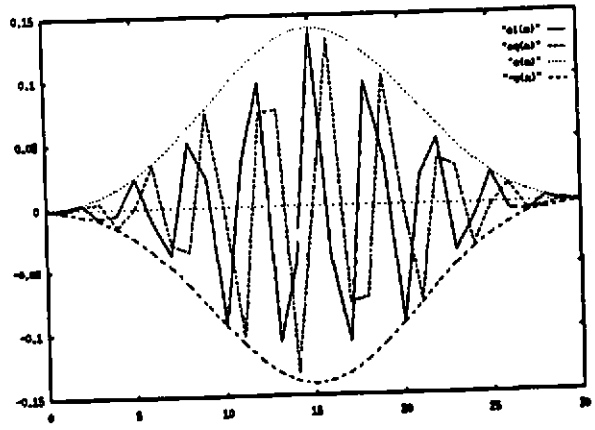

Fig 1b. In-phase and quadrature match-filtered pulse, with envelope (centre 31 samples only)

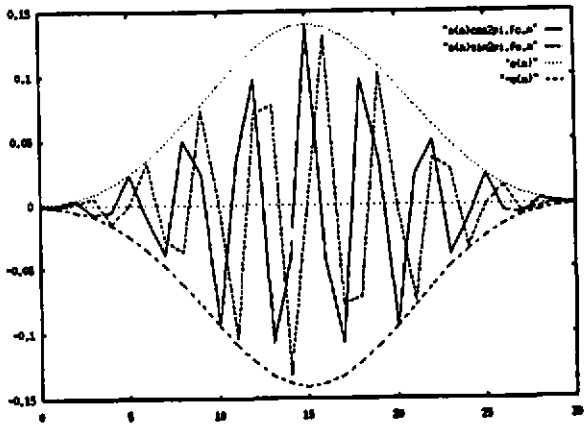

Fig 1c. Sampled centre-frequency cos and sin waveforms modulated by envelope

WIDEBAND SYNTHETIC-APERTURE IMAGING IN GROUND COORDINATES USING A DIGITAL PHASED-ARRAY TECHNIQUE

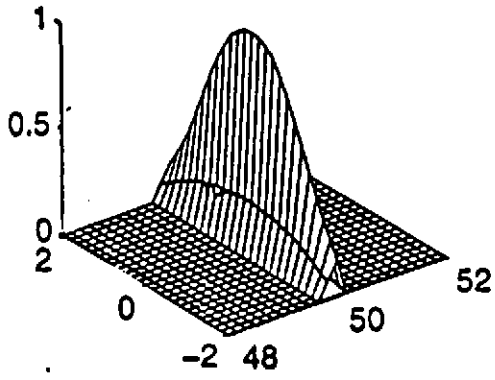

Fig 2. Point-spread-function for chirp pulse of Fig 1a, $\tau=2\mu$, $f_c=150$ kHz echoed by reflector at 50 m and received by 1 m long, 32 element, array.

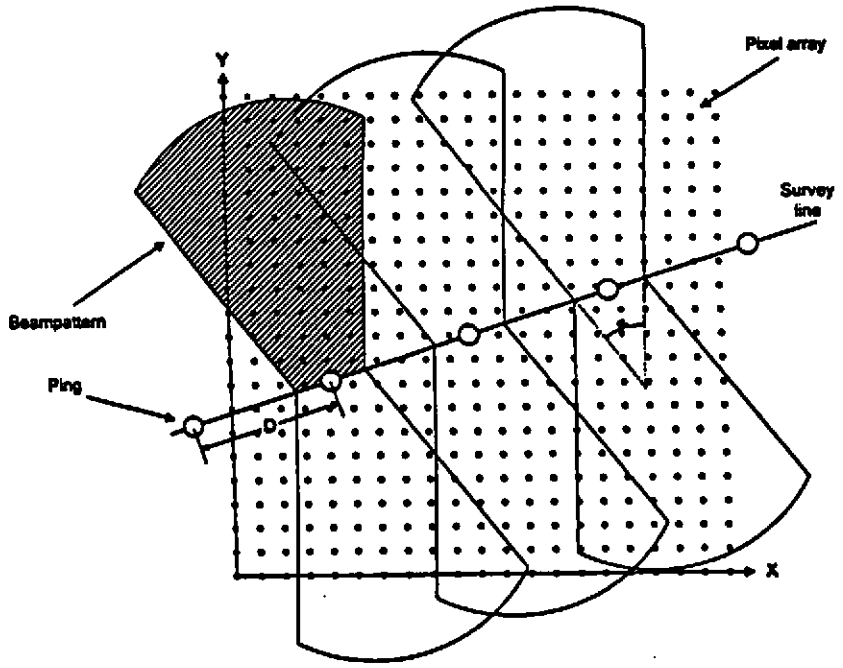

Fig 3. Simplified plan view of sidescan survey using sector imaging

WIDEBAND SYNTHETIC-APERTURE IMAGING IN GROUND COORDINATES USING A DIGITAL PHASED-ARRAY TECHNIQUE

Fig 4. Phase-Dependant Synthetic-Aperture PSF corresponding to Fig 2.

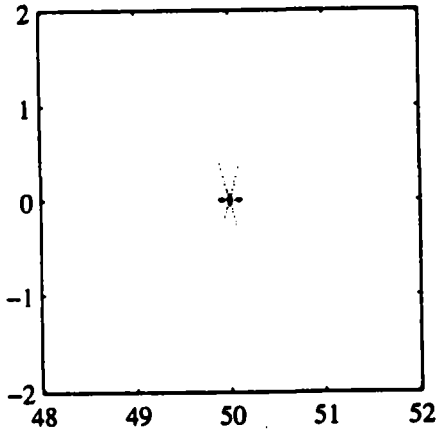

Fig 4a. Intensity Plot

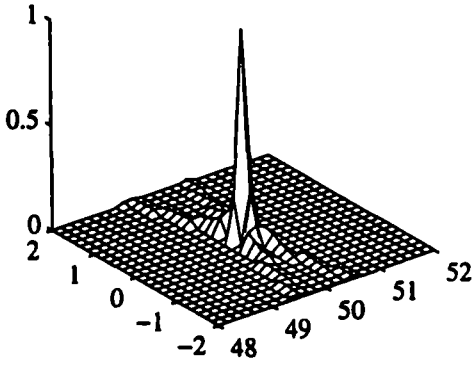

Fig 4b. Isometric Plot

Fig 5. Phase-Independant Synthetic Aperture PSF corresponding to Fig 2.

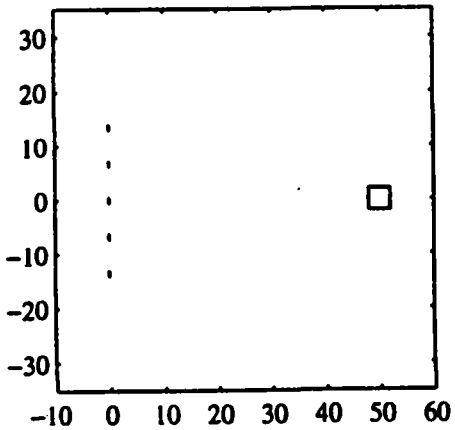

Fig 5a. Scenario

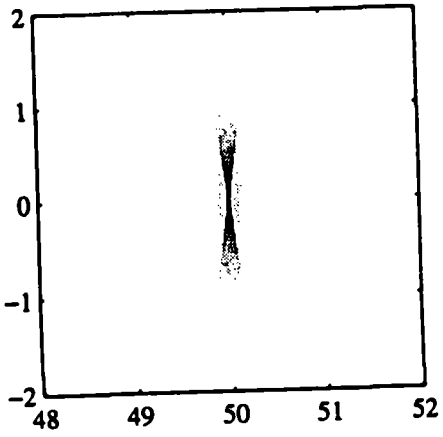

Fig 5b. Intensity Image

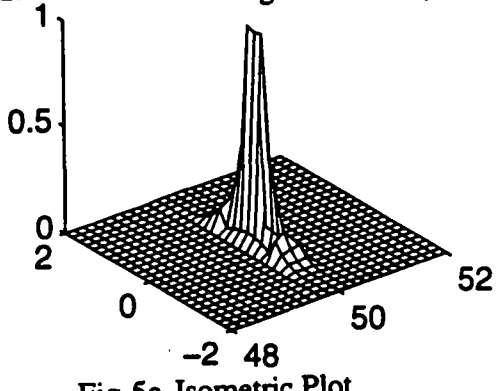

Fig 5c. Isometric Plot